ELSEVIER

Ceramics International 30 (2004) 1059–1065

CERAMICS INTERNATIONAL

www.elsevier.com/locate/ceramint

Machinable spodumene–fluorophlogopite glass ceramic

Emad M. El-Meliegy

Department of Ceramics, National Research Centre, 12622 El-Tahrir Street, Dokki, Cairo, Egypt

Received 9 September 2003; received in revised form 19 September 2003; accepted 17 November 2003

Available online 10 March 2004

Abstract

Simultaneous crystallization of fluorophlogopite and beta-spodumene solid solutions is adjusted to achieve machinable porcelain with low expansion coefficient for dental application. The crystallization is guided by the thermal behavior to achieve the desired properties. The beta-spodumene phase tends to harden the body and thereby impair the machinability character when its proportion approaches more than 50%. An expansion coefficient $< 40 \times 10^{-7}\,^{\circ}C^{-1}$ with good machinability is achieved by adjusting the content of beta-spodumene. The rate of heating slightly above the transformation range ought not to be so rapid to achieve sufficient grain growth. Heating rates of 10 °C/min or higher is successfully employed to achieve the desired porcelain.

Keywords: Fluorophlogopite; Beta-spodumene; Machinability; Low expansion coefficient

1. Introduction

Considerable research has been directed to porcelain bodies demonstrating excellent high temperature dimensional stability together with good machinability [1,2]. Most naturally occurring micas have hydroxyl group in a silicate composition, whereas micas produced synthetically often involves fluorine substituted in the body structure in place of the hydroxyl groups [3]. Thus, synthetic micas have frequently been termed as fluorophlogopite solid solutions or fluormicas. Fine-grained, polycrystalline mica ceramics do not demonstrate excellent flexibility, but on the other hand, exhibit good dielectric behavior, thermal stability, and good machinability [4–6].

One fundamental shortcoming in all of the synthetic fluormicas is their high coefficient of thermal expansion $> 90 \times 10^{-7}\,^{\circ}C^{-1}$ with consequent poor resistance to thermal shock [7–12]. Therefore, there has been a need for a product demonstrating good machinability character of mica, but with a much lower coefficient of thermal expansion [12–14].

Beta-spodumene is a trapezohedral form of the tetragonal system with a classical formula $Li_2O{\cdot}Al_2O_3{\cdot}4SiO_2$, and is a high temperature form of alpha-spodumene. Beta-spodumene results from heating alpha-spodumene to a conversion temperature of 700 °C. Beta-spodumene has low expansion coefficient and high hardness. The simultaneous crystallization of beta-spodumene with fluorophlogopite enhances the mechanical properties and the thermal shock resistance through reducing the thermal expansion coefficient [15–22].

The present work aims at the preparation of porcelain containing synthetic fluorophlogopite as the primary mineral phase, which lends the porcelain good machinability. A simultaneous crystallization of beta-spodumene solid solution with fluorophlogopite will reduce the overall coefficient of thermal expansion and improve the hardness. In sum, the porcelain is machinable with low thermal expansion and each phase contributes distinctive characteristics.

2. Experimental procedures

Egyptian feldspar with a chemical composition shown in Table 1 was used to prepare spodumene–fluorophlogopite porcelains. The composition of the mixes is satisfied using chemicals including MgF_2 (Fluka), boric acid (Fluka), Li_2CO_3 (Aldrich), K_2CO_3 (Aldrich). Three mixes were prepared containing 10, 30, and 60% spodumene on the extent of fluorophlogopite corresponding to F_1, F_3, and F_6, respectively. The chemical compositions of the different mixes are demonstrated in Table 2.

E-mail address: emadmeliegy@hotmail.com (E.M. El-Meliegy).

0272-8842/$30.00 © 2004 Published by Elsevier Ltd and Techna Group S.r.l.
doi:10.1016/j.ceramint.2003.11.009

Table 1
Chemical analysis of feldspar

Oxide (wt.%)	
K_2O	11.70
Al_2O_3	18.40
SiO_2	64.03
Na_2O	01.60
Fe_2O_3	00.49
CaO	02.70
TiO_2	00.02
LOI	01.00

Table 2
Chemical composition of the different mixes

Oxide (wt.%)	F_1	F_3	F_6
Li_2O	0.80	2.41	4.82
K_2O	10.05	7.82	4.47
MgO	17.24	13.41	7.66
Al_2O_3	13.65	16.71	21.30
SiO_2	36.94	42.29	47.83
MgF_2	13.32	10.36	5.92
B_2O_3	8.00	8.00	8.00

B_2O_3 was added to the mixes on the extent of silica percentage.

Batches were milled and mixed in a ball mill for 1 h. The milled powders were uniaxially pressed into 100 g cubes under a force of 100 MPa. The pressed cubes were calcined at 1000 °C/1 h. The calcined cubes were fused in platinum dishes using a fast firing furnace at temperatures between 1100 and 1400 °C. The fused materials were poured in a stream of cold water to form frits. Frits were milled for 4 h to pass 75 μm sieve.

The milled powders were thermally analyzed via DTA using apparatus type Bähr 701 at a rate of 5 °C/min up to 1100 °C. The powders were pressed into small rectangular samples of 12 mm length and 6 mm width under 100 MPa to be used for thermal expansion determination. The pressed samples were heat treated at 650 °C/3 h and then at 950 °C for 2 h. The expansion behavior of the processed samples was studied via dilatometer type Bähr 801 up to 1000 °C with a heating rate of 5 °C/min.

Frit powders were pressed into 10 mm diameter and 5 mm height cylindrical samples under 100 MPa. The pressed samples were heat treated at 650 °C/2 h. Different groups of the treated samples were then fired between 900 and 1050 °C. The phase composition of samples processed at 900 and 1000 °C was followed by XRD analysis. XRD analysis was carried out using apparatus type Brouckur D8 advance with Cu-target and Ni-filter.

Samples of the different mixes were embedded into polymer resin and polished using different grades of abrasives followed by 1.0 μm diamond paste. The polished specimens were washed by water and acetone in an ultrasonic bath several times. The polished samples were chemically etched using a mixture containing 1% EDTA and 5% NaOH for 60 s. The etched samples were washed carefully with distilled water. Gold layer of 3 μm thickness was sputtered over the polished surface. The microstructure of the coated samples was analyzed via SEM type JSM-6400 operating at 20 KV attached with EDAX unit

Some of the polished samples, washed carefully with acetone and water, were coated with gold without etching. Vickers microhardness was determined through indentation.

3. Results and discussion

The manufacture of frit porcelain involves three fundamental steps. The first is the melting of a glass-forming batch normally containing a nucleating agent. The second is the cooling of the melt at a sufficiently rapid rate in a stream of cold water. The third is heat treatment of the processed frit to be crystallized in situ [1–6].

Normally the crystallization is performed in two stages. Thus, the glass body is initially heated to a temperature slightly above the transformation range to develop nuclei in the glass body. The nuclei provide sites for subsequent crystal growth. The nucleated frit body is heated to a temperature above the softening point of the porcelain to enhance the growth of crystals on the nuclei [10,11].

The crystallization mechanism leads to a substantially simultaneous growth of crystals on numerous nuclei.

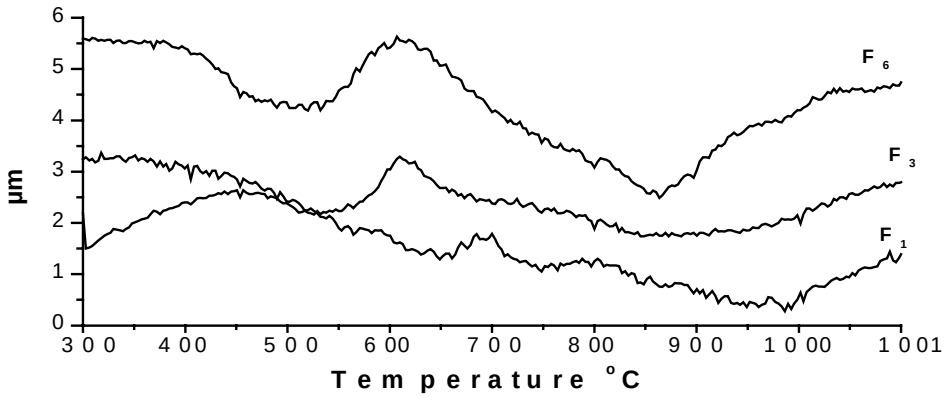

Fig. 1. DTA results of the different mixes.

Accordingly, porcelain conventionally consists of uniformly fine-grained crystals randomly oriented and homogeneously dispersed, throughout a residual glassy matrix. The physical properties exhibited by porcelain are related to the developed phases than to the glassy phase. The crystallization mechanism provides porcelains, which are free from voids [10,12].

In the current work, fluorophlogopite constitutes the primary mineral phase together with beta-spodumene solid solution, in addition to substantial amounts of forsterite as secondary mineral phases The crystallization of the aforementioned phases are guided by the thermal behavior shown in Fig. 1. The exothermic peaks occurring at 580, 600, and 610 °C of F_1, F_3, and F_6, respectively, related to the crystallization of spodumene. On the other hand, two exothermic peaks occurring at 700 and 800 °C in mix F_1 relate to the transformation of alpha-spodumene to beta-spodumene and the crystallization of fluorophlogopite, respectively. Other three exothermic peaks occurring at 860, 900, and 980 °C of F_1, F_3, and F_6, respectively, relate to melting.

The respective porcelain contains synthetic fluorophlogopite as the primary mineral phase that lends good machinability and electrical insulating properties; wherein a substantial amount of beta-spodumene solid solution crystals is included to reduce the overall coefficient of thermal expansion. In sum, a multiphase porcelain is created and each phase contributes distinctive characteristics. The final mineral assemblages displayed by XRD patterns in Figs. 2 and 3 comprise fluorophlogopite solid solution and beta-spodumene solid solution homogeneously dispersed within a glass matrix.

The attached SEM micrographs clearly portray the large fluorophlogopite crystals and interstitial beta-spodumene solid solution grains. Beta-spodumene is extremely fine-grained with grains having diameters less than about 1 μm and difficult to differentiate visually. Nevertheless, the presence of beta-spodumene solid solution is confirmed by XRD and DTA analyses.

The large plate-like and tabular grains are fluorophlogopite. The best machinability is secured at the highest concentrations of fluormica wherein the fluorophlogopite has

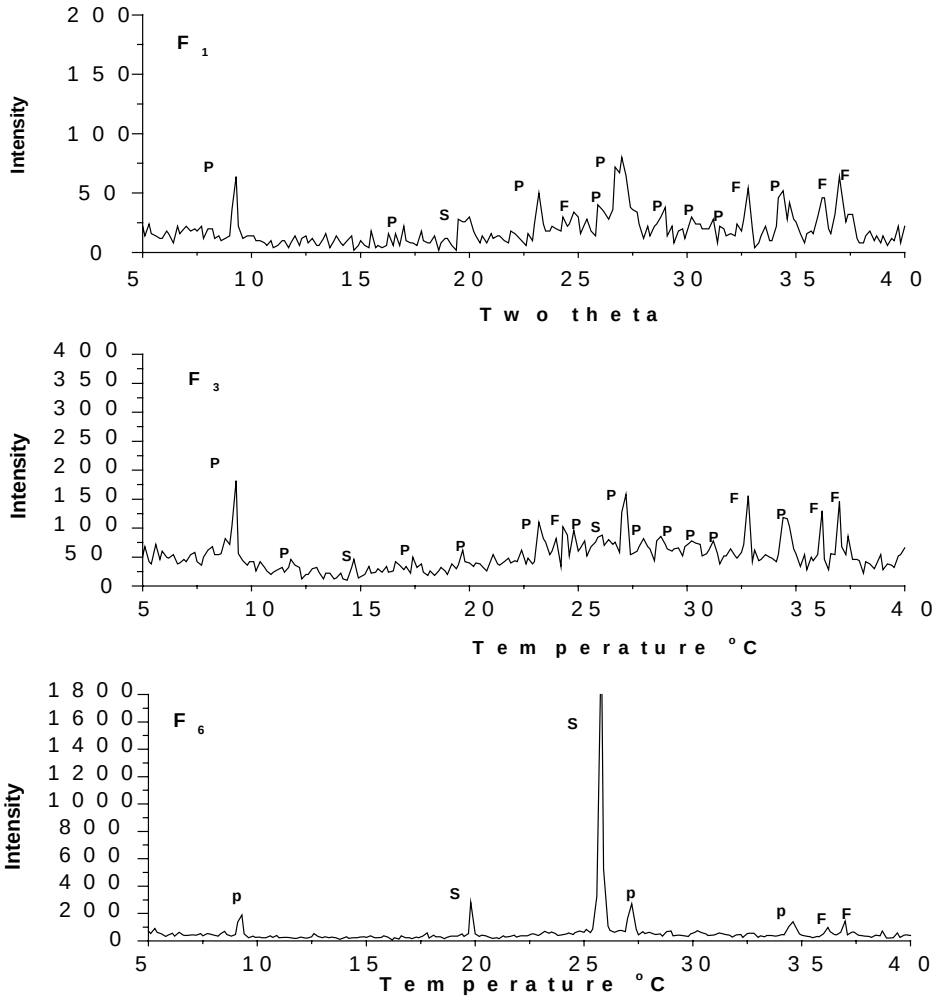

Fig. 2. XRD analysis of the mixes fired at 1000 °C. P, fluorophlogopite; S, beta-spodumene; F, forsterite.

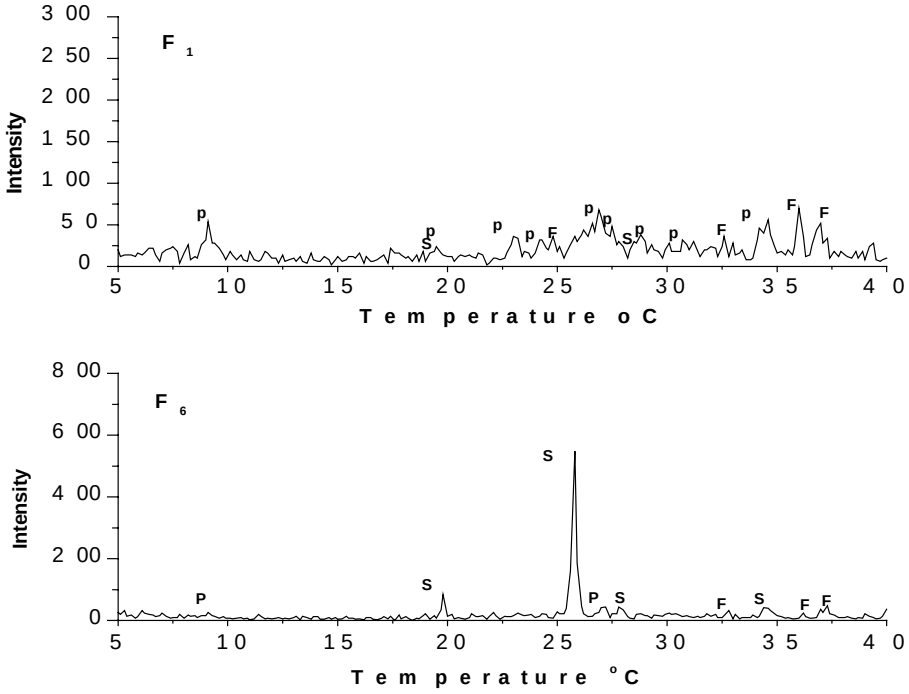

Fig. 3. XRD analysis of the mixes fired at 900 °C.

a grain size of less than 5 μm. Fluorophlogopite forms the major phase in both F_1 and F_3 mixes as shown in Figs. 4 and 5. Mica grains are uniform in size and are randomly distributed in the glass matrix. Beta-spodumene phase occurs in a considerable amount in both as F_1 and F_3, but its content does not permit reliable decrease in the expansion or further increase in the value of hardness. Nevertheless, such bodies F_1 and F_3 exhibit coefficients of thermal expansion of 36×10^{-7} and $31 \times 10^{-7}\,^{\circ}C^{-1}$, respectively. Hence, the presence of beta-spodumene solid solution enables lower expansion coefficient to demonstrate excellent resistance to thermal shock.

Beta-spodumene increases in mix F_6 as displayed by the SEM results in Fig. 6, but to a limit impair the machinability, perform excessive increase in the hardness and demonstrate a value of expansion coefficient $-27 \times 10^{-7}\,^{\circ}C^{-1}$. Thus, the singular interlocking microstructure of the plate-like or tabular fluormica crystals allow thermal expansion adjustment and respective shrinkage.

The microstructure of the body also affects the strength. Spherulitic or dendrite growths of mica result in the production of weak bodies. The interlocking of the fluorophlogopite crystals coupled with a relatively high percentage of fine-grained beta-spodumene solid solution, promotes the highest mechanical strength., reduce the expansion coefficient to less than $35 \times 10^{-7}\,^{\circ}C^{-1}$ compared with the expansion coefficient of mica; $90 \times 10^{-7}\,^{\circ}C^{-1}$.

In the current work, no nucleating agent is normally employed. The high content of MgO and F is adequate to allow amorphous phase separation and subsequent internal nucleation of both fluorophlogopite and spodumene solid solution. Thus, the inclusion of nucleating agents as TiO_2 and/or ZrO_2, normally utilized to nucleate beta-spodumene solid solution crystals is not necessary in the current mixes. The crystallization of the respective phases is performed in a desired way without nucleating agents and perhaps the presence of specific mineralizers encourages the development of parasitic phases. On the other hand, addition of B_2O_3 is an important factor for the crystallization of fluorophlogopite exhibiting good mechanical machinability. Volatilization of fluoride from the melt was quite low at the melting temperatures employed.

The developed beta-spodumene phase tends to harden the body and thereby impair the machinability character according to their amount, growth and distribution in the glassy matrix. However, to achieve a coefficient of expansion of less than $40 \times 10^{-7}\,^{\circ}C^{-1}$, beta-spodumene solid solution should comprise at least about 25% of the total crystallinity as shown by F_1 and F_3. Therefore, when the proportion of beta-spodumene solid solution approaches more than 50%, the hardness increases sharply and the porcelain is no longer to be considered machinable as demonstrated by F_6 fired at 1000 °C. The hardness of the mix F_6 fired at temperature >950 °C sharply increase indicating the machinability deterioration. The two mixes F_1 and F_3 are shown to be readily machinable porcelains at all temperature ranges. The hardness values generally increase with the increase in temperature or the amount of beta-spodumene as shown in Table 3.

Beta-spodumene solid solution comprised the primary crystal phase of F_6 with a substantial amount of

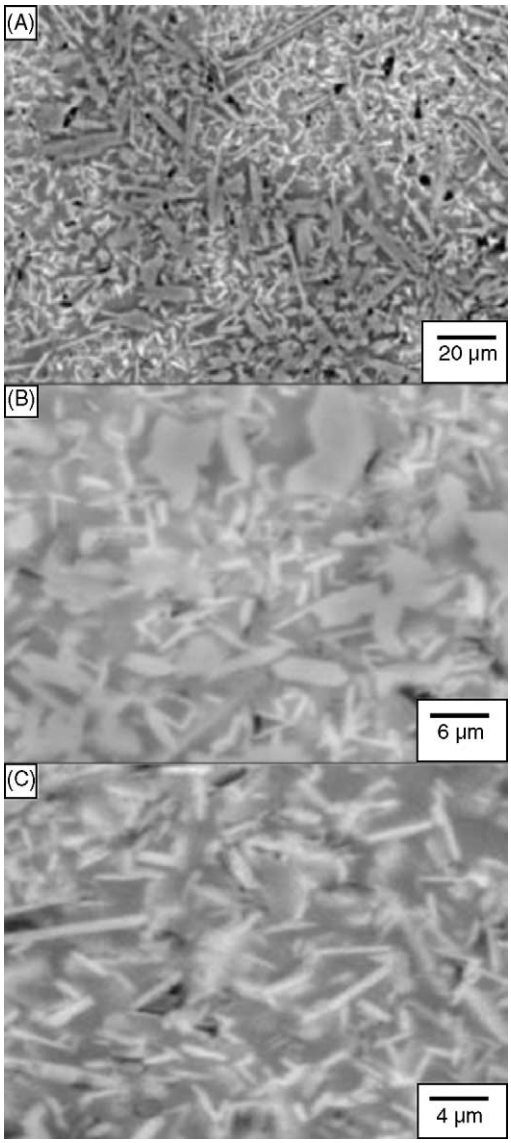

Fig. 4. SEM results of F_1 fired at 950 °C.

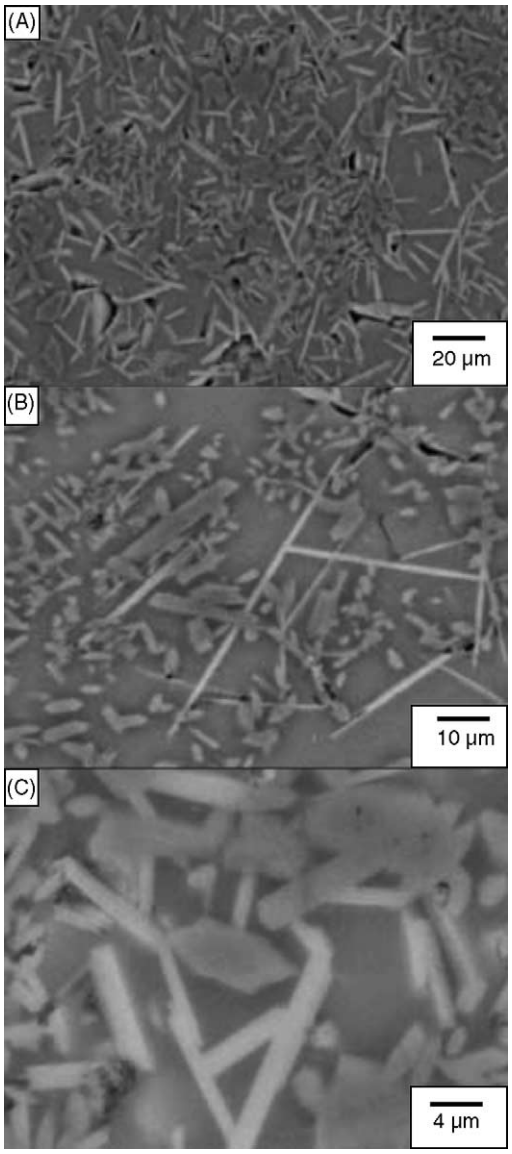

Fig. 5. SEM results of F_3 fired at 950 °C.

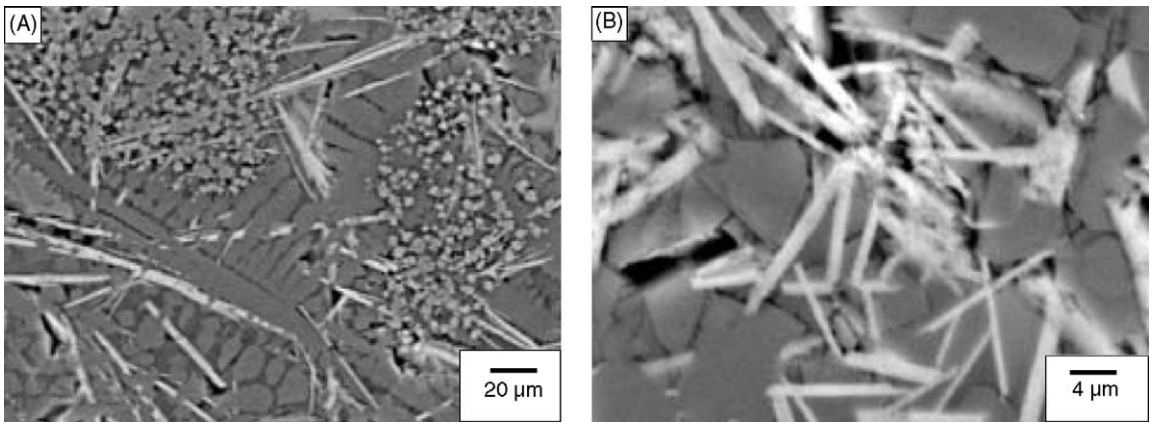

Fig. 6. SEM results of F_6 fired at 950 °C.

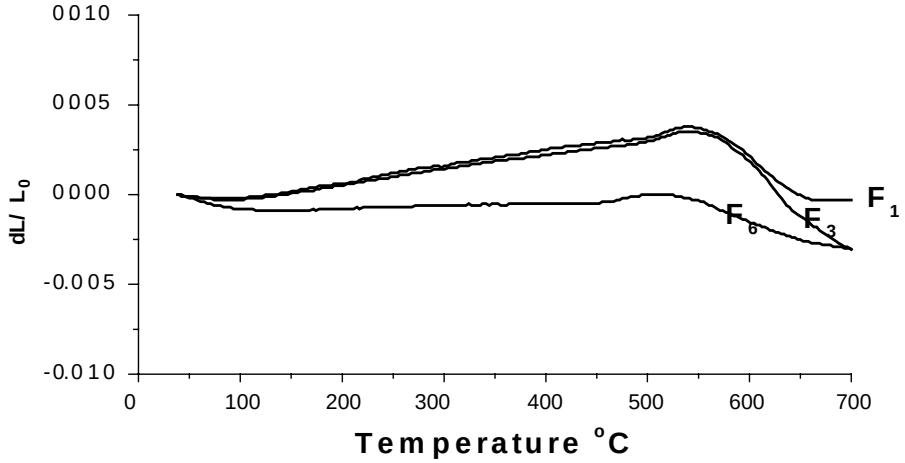

Fig. 7. Thermal expansion results of the different mixes.

Table 3
Microhardness results of the different mixes

Temperature (°C)	Microhardness values (kg/mm^2)		
	F_1	F_3	F_6
850	50.70	53.90	101.00
900	62.00	96.60	110.20
950	113.50	118.10	117.50
1000	75.60	168.80	217.00
1050	80.40	132.90	689.70
1100	95.60	105.50	911.00

fluorophlogopite. Oxides such as MgO and B_2O_3 are present in the compositions. Their presence assures the formation of fluorophlogopite phase with beta-spodumene. The formation of parasitic forsterite phase is controlled by the ratio of $MgO + MgF_2/SiO_2$ either during the normal heat treatment or during a subsequent prolonged exposure to high temperatures.

The rate of crystal growth is dependent upon the heat treatment regime. Hence, at temperatures slightly above the transformation range, crystal growth is quite slow and the glass body is subject to deformation. Therefore, the heating rate for the porcelain at temperatures above the transformation range ought not to be so rapid as to achieve adequate time sufficient to appropriate grain growth. Heating rates of 10 °C/min or higher is successfully employed. The use of the two-step crystallization is preferred to minimize the deformation, since substantial nucleation insures more rapid and uniform subsequent crystallization. The current bodies are heat treated at 650 °C/3 h before crystallization at temperatures between 900 and 1050 °C to insure uniform subsequent crystallization.

In the current work, it was found that the porcelain bodies exhibit average coefficients of thermal expansion of less than $40 \times 10^{-7}\,°C^{-1}$ (20–700 °C). The thermal expansion results are displayed in Fig. 7. The transformation temperatures are 510, 510, and 460 °C and the softening points are 550, 550, and 520 °C for F_1, F_3, and F_6, respectively. The expansion coefficients of the different mixes are 36.21, 31.03, and −27.60 for F_1, F_3, and F_6, respectively. A distinct similarity is apparent in the expansion behavior of both F_1 and F_3. The two samples showed closely matched expansion behavior.

4. Conclusion

1. Beta-spodumene simultaneously crystallizes with fluorophlogopite in all mixes at different temperatures.
2. The porcelain is no longer readily machinable on approaching more than 50% beta-spodumene.
3. Good machinability and low expansion coefficient are achieved in mixes containing less than 25% beta-spodumene together with fluorophlogopite.
4. The porcelain requires heat treatment within the transformation range with a heating rate of 10 °C/min or higher and is successfully employed to achieve subsequent crystallization.

References

[1] W. Höland, W. Vogel, K. Naumann, J. Jummel, Interface reactions between machinable bioactive glass-ceramics and bone, J. Biomed. Mater. Res. 19 (1985) 303–312.
[2] D.G. Grossmann, Machinable glass ceramics based on tetrasilicic mica, J. Am. Ceram. Soc. 55 (9) (1972) 446–449.
[3] W. Deer, R. Howie, J. Zussman, An Introduction to Rock Forming Minerals, Longman Group Ltd., UK, 1966.
[4] S.N. Hoda, G.H. Beal, Alkaline Earth Mica Glass-Ceramics, Advances in Ceramics, Vol. 4: Nucleation and Crystallization in Glasses, American Ceramic Society, 1982, pp. 287–299.
[5] P.A. Tick, Zirconium–alkali fluorophosphate glasses, Phys. Chem. Glasses 23 (5) (1982) 73–76.
[6] W. Eitel, R.A. Hatch, M. Denny, Synthetic mica investigations: II. Role of fluorides in mica batch reactions, J. Am. Ceram. Soc. 36 (10) (1953) 341–348.
[7] B. Yu, K. Liang, S. Gu, Effect of the microstructure on the mechanical properties of $CaO–P_2O_5–SiO_2–MgO–F^-$ glass ceramics, Ceram. Int. 29 (6) (2003) 695–698.

[8] M. Goswami, A. Sarkar, T. Mirza, V. Shrikhande, K. Sangeeta, G. Kothiyal, Study of some thermal and mechanical properties of magnesium aluminium silicate glass ceramic, Ceram. Int. 28 (6) (2002) 585–592.
[9] D. Ibrahim, E. El-Meliegy, Mica leucite dental porcelain, Br. Ceram. Trans. 100 (6) (2001) 260–264.
[10] E.A. Mustafa, Fluorophlogopite porcelain based on talc–feldspar mixture, Ceram. Int. 27 (1) (2001) 9–14.
[11] T. Hoche, S. Habelitz, I. Khodos, Origin of unusual fluorophlogopite morphology in mica glass-ceramics of the system SiO_2–Al_2O_3–MgO–K_2O–Na_2O–F_2, J. Crystal Growth 192 (1) (1998) 185–195.
[12] C. Xiaofeng, L. Hench, D. Greenspan, Z. Jipin, Z. Xiaokai, Investigation on phase separation, nucleation and crystallization in bioactive glass-ceramics containing fluorophlogopite and fluorapatite, Ceram. Int. 24 (5) (1998) 401–410.
[13] M. Wang, N. Wu, S. Yang, S.-B. Wen, Morphology and microstructure in the sintering of β-spodumene precursor powders with TiO_2 additive, J. Eur. Ceram. Soc. 23 (3) (2003) 437–443.
[14] E. Suzdal'tsev, Glass ceramics of β-spodumene composition with controlled dielectric constant, Refractories Ind. Ceram. 43 (6) (2002) 176–178.
[15] M. Wang, S. Yang, S. Wen, N. Wu, Sintering Li_2O–Al_2O_3–$4SiO_2$ precursor powders with ultrafine TiO_2 additives, Mater. Chem. Phys. 76 (2) (2002) 162–170.
[16] A. El-Shennawi, E. Hamzawy, G. Khater, A. Omar, Crystallization of some aluminosilicate glasses, Ceram. Int. 27 (7) (2001) 725–730.
[17] P. Riello, P. Canton, N. Comelato, S. Polizzi, M. Verita, G. Fagherazzi, H. Hofmeister, S. Hopfe, Nucleation and crystallization behavior of glass-ceramic materials in the Li_2O–Al_2O_3–SiO_2 system of interest for their transparency properties, J. Non-Cryst. Solids 288 (1) (2001) 127–139.
[18] L. Arnault, M. Gerland, A. Rivière, Microstructural study of two LAS-type glass-ceramics and their parent glass, J. Mater. Sci. 35 (9) (2000) 2331–2345.
[19] G. Helsch, J. Günster, G. Frischat, K. Helming, B. Roling, S. Murugavel, Preparation, characterization and properties of textured glass ceramics in the system Li_2O–Al_2O_3–SiO_2, Phys. Chem. Glasses 44 (1) (2003) 19–25.
[20] I. Low, E. Mathews, T. Garrod, D. Zhou, D. Phillips, X. Pillai, Processing of spodumene-modified mullite ceramics, J. Mater. Sci. 32 (14) (1997) 3807–3812.
[21] A. Nordmann, Y. Cheng, Crystallization behavior and microstructural evolution of a Li_2O–Al_2O_3–SiO_2 glass derived from spodumene mineral, J. Mater. Sci. 32 (1) (1997) 83–89.
[22] Y. Sung, Mechanical properties of cordierite and β-spodumene glass-ceramics prepared by sintering and crystallization heat treatments, Ceram. Int. 23 (5) (1997) 401–407.